



**HAL**  
open science

## Studies on catalytic and structural properties of BaRuO<sub>3</sub> type perovskite material for diesel soot oxidation

Pradeep Doggali, Fabien Grasset, Olivier Cador, S. Rayalu, Yasutake Teraoka, Nitin Labhsetwar

### ► To cite this version:

Pradeep Doggali, Fabien Grasset, Olivier Cador, S. Rayalu, Yasutake Teraoka, et al.. Studies on catalytic and structural properties of BaRuO<sub>3</sub> type perovskite material for diesel soot oxidation. Journal of Environmental Chemical Engineering, 2014, 2, pp.340-343. 10.1016/j.jece.2014.01.002 . hal-00974714

**HAL Id: hal-00974714**

**<https://hal.science/hal-00974714>**

Submitted on 2 Jun 2014

**HAL** is a multi-disciplinary open access archive for the deposit and dissemination of scientific research documents, whether they are published or not. The documents may come from teaching and research institutions in France or abroad, or from public or private research centers.

L'archive ouverte pluridisciplinaire **HAL**, est destinée au dépôt et à la diffusion de documents scientifiques de niveau recherche, publiés ou non, émanant des établissements d'enseignement et de recherche français ou étrangers, des laboratoires publics ou privés.

1 **Studies on catalytic and structural properties of BaRuO<sub>3</sub> type perovskite**  
2 **material for diesel soot oxidation**

3 **Pradeep Doggali, F. Grasset<sup>a</sup>, O. Cador<sup>a</sup>, S. Rayalu, Y. Teraoka<sup>b</sup> and Nitin Labhsetwar\***

4  
5 CSIR- National Environmental Engineering Research Institute,  
6 (CSIR-NEERI), Nehru Marg, Nagpur, 440020 India

7 <sup>a</sup>UMR Science Chimiques de Rennes UR1-CNRS 6226, Université de Rennes 1, Campus de  
8 Beaulieu, CS74205, F-35042 Rennes Cedex (France)

9 <sup>b</sup>Department of Energy and Material Sciences, Faculty of Engineering Sciences, Kyushu  
10 University, Kasuga, Fukuoka 816-8580, Japan

11  
12 \* Author for correspondence: E-mail: nk\_labhsetwar@neeri.res.in

13 Tel: 0091-712-2249885-90; Fax: 0091-712-2249900

14 Postal address:

15 Dr. Nitin Labhsetwar,  
16 Senior Principal Scientist,  
17 CSIR-National Environmental Engineering Research Institute (CSIR-NEERI)  
18 Nehru Marg, NAGPUR-440020, India

23  
24  
25  
26  
27  
28  
29  
30  
31  
32  
33  
34  
35  
36  
37  
38  
39  
40  
41  
42  
43  
44  
45

## Abstract

BaRuO<sub>3</sub> based perovskite type catalytic material was synthesized by co-precipitation method and its catalytic activity has been tested for diesel soot oxidation. This material shows high catalytic activity for carbon/soot oxidation reaction with lowering of carbon oxidation temperature by >190 °C. The catalytic activity could be due to dissociative adsorption of oxygen on BaRuO<sub>3</sub> surface. It is postulated by structural investigations that 120 planes of BaRuO<sub>3</sub> can have abundant Ru atoms which, can facilitate the oxygen dissociation. The additional advantage of using Ru in BaRuO<sub>3</sub> is the thermal stability of Ru in oxide matrix as well as basicity offered by Ba. These synergetic effects can also be responsible for the high soot/carbon oxidation activity of this perovskite type material, which can be a potential candidate for control of soot emissions from combustion processes and vehicle exhaust.

**Key words:** *BaRuO<sub>3</sub>, perovskite, diesel soot oxidation, vehicular exhaust emission control.*

46 **1. Introduction**

47 Particulate matter (PM) emissions from diesel engines are harmful due to both their chemical  
48 composition and particle size [1, 2]. The diesel particulate filter (DPF) has so far been the most  
49 potential technological option for the effective control of diesel PM emissions, however, its  
50 regeneration possibly at the exhaust temperature appears to be the only but difficult limitation.  
51 Although, NO<sub>x</sub> based catalyst assisted passive regenerative type DPFs have been developed,  
52 soot oxidation by oxygen/air remains focus of intense research to avoid the NO<sub>x</sub> dependency for  
53 regeneration. Considerable success has been achieved in development of new catalytic materials  
54 and the possible mechanisms for the direct soot oxidation by oxygen [3, 4]. As diesel exhaust  
55 temperature is substantially lower than the soot oxidation light-off temperature, development of  
56 active catalytic materials is still a challenging issue and demand for the investigations on new  
57 catalytic materials. Ruthenium in its metallic, coordinated and oxide forms is a good catalytic  
58 material for several reactions of commercial and environmental importance [5, 6]. It is an  
59 excellent oxidation catalyst [7]. Nevertheless, its catalytic applications for high temperature  
60 oxidation reactions and automobile exhaust treatment could not find much practical success  
61 mainly due to its relatively inferior thermal stability. Ruthenium dioxide (RuO<sub>2</sub>) has a tendency  
62 to get oxidized in to higher oxides, which are of volatile nature at temperature beyond 800°C [8].  
63 This has often been a limitation for its high temperature applications, including catalytic  
64 applications. Also, there are very limited tailoring possibilities with RuO<sub>2</sub> to alter its catalytic  
65 properties for specific reactions. Ruthenium can be stabilized in ABO<sub>3</sub> type perovskite material  
66 structure, which offers good thermal stability as well as catalytic material properties due to its  
67 structural and chemical specifications [9].

68 With more reliable findings on effective dissociative adsorption of oxygen on Ru surface,  
69 the interest in catalytic properties of Ru based materials has been rejuvenated for academic as well  
70 as practical reasons [10]. BaRuO<sub>3</sub>, one of the relatively simple and stable Ru based oxides,  
71 crystallizes in hexagonal perovskite material structure consisting of face sharing octahedra [11].  
72 The hexagonal BaRuO<sub>3</sub> provides an example of the complex oxide based on closed packed stacking  
73 of BaO layers of perovskite type material structure. The physical properties of BaRuO<sub>3</sub> compound  
74 are mainly due to unfilled 4 d level of Ru ions, however, the ionic radii of Ba cation also play a  
75 significant role [11]. Presence of ruthenium in 4+ stable oxidation state and possible influence of  
76 Ba on the catalytic active Ru makes this compound a potential material for catalytic studies. The  
77 properties of ruthenium based perovskite type materials for their catalytic applications have been  
78 seldom investigated, although theoretically they can be potential catalytic materials for various  
79 reactions including oxidation reactions. We have been successful in development of new and  
80 improved methods for the synthesis of lanthanum based perovskite type ruthenate materials, which  
81 show high thermal stability and catalytic properties [9, 12-14]. As ruthenium is relatively much  
82 cheaper (about 18 times than Pt, 10 times than Pd and 12 times to that of Rh) metal than other  
83 Platinum Group Metals (PGM), its use in auto-exhaust emission control can be justified.

84 In this work, we report the catalytic properties of BaRuO<sub>3</sub> type perovskite material with high  
85 catalytic activity for carbon/soot oxidation reaction, probably for the first time. It was possible to  
86 understand certain structure-property relations through the structural models as well as the chemical  
87 composition of this material. The activity and stability results of BaRuO<sub>3</sub> can help rejuvenating  
88 ruthenium based perovskites for important applications in environmental catalysis.

## 89 **2. Experimental**

### 90 **2.1. Synthesis of BaRuO<sub>3</sub>**

91 Co-precipitation has been widely used for the synthesis of a large number of perovskites. In  
92 the present method, Ba<sup>2+</sup> and Ru<sup>3+</sup> precursors were dissolved in deionized water and subsequently  
93 mixed together. The mixed metal ion solution was slowly added with constant stirring, to aqueous  
94 mixed alkali solution. A mixed alkali solution was prepared by mixing 500 ml each of 1M aqueous  
95 ammonium carbonate solution and 500 ml of 1 N aqueous ammonia solution. The precipitate thus  
96 obtained was allowed to settle for 5 h followed by filtration and washings with de-ionized water  
97 and oven drying at 70 °C. The resultant mass was heated at 500 °C for 5 h followed by grinding and  
98 further heating at 800 °C for 6 h.

## 99 **2.2. Characterization**

100 XRD patterns were recorded on a Rigaku Rint-220HF diffractometer, operated at 40 kV and  
101 50 mA with a monochromator and using Cu K $\alpha$  radiations ( $\lambda = 0.15418$  nm). Indexing of XRD  
102 peaks was done, by using JCPDS database for the respective phases. Surface area was measured by  
103 nitrogen adsorption method using automatic gas adsorption apparatus BELSORP 28SA (produced  
104 by Nippon Bell Co.) and data were evaluated by BET method. The samples were pre-treated at 300  
105 °C before the nitrogen adsorption experiments. Thermal stability experiments were performed by  
106 heating the material at 900 °C, under air atmospheres and also performed using TGA technique  
107 (Rigaku-TAS-200 apparatus) in the same temperature range, mainly to study the possibility of  
108 thermal loss by the formation of volatile ruthenium oxides.

## 109 **2.3. Catalytic Evaluations**

110 The synthesized BaRuO<sub>3</sub> was evaluated for its carbon/soot oxidation activity following a  
111 batch type temperature programmed reaction procedure using activated carbon. 100 mg of carbon-  
112 catalyst (ca. 5wt%) mixture was homogenized in an agate lines mortar pestle, pelletized (tight  
113 contact condition) and sieved to 20-100 mesh. The pellets were placed in a fixed bed flow reactor

114 with a programmable heater controller. A gas mixture containing 15 % oxygen was flown with the  
115 increasing temperature with a predetermined heating cycle. Gas analysis was carried out using an  
116 auto-sampling PC controlled, MTI-P-200, Shimadzu GC system with molecular sieve and Porapak-  
117 Q and molecular sieve columns. The activation energy has been estimated by using Ozawa method  
118 by proper interpretation of TGA data. The thermo gravimetric analysis experiments were performed  
119 under loose contact condition wherein the mixture of soot and catalysts were heated from 35 to  
120 800°C at different heating rates, in air atmosphere. According to the Ozawa Method, the following  
121 relationship links the values of the heating rate  $\ln(\phi)$  with the corresponding values of temperature  
122 ( $T_\alpha$ ) at which a fixed fraction of carbon is burned during each run;

$$123 \quad \ln(\phi) = 1.052(E/R) (1/T_\alpha) + A$$

124 Where, A is a constant, E is activation energy ( $\text{kJ mole}^{-1}$ ) and R is ideal gas constant ( $8.314 \text{ J/}$   
125  $\text{mole/K}$ ) [15, 16]. In this case, TGA experiments were performed using the loose contact method by  
126 shaking the mixture of catalyst and carbon (90:10) in a glass bottle for five minutes. This method is  
127 often used as a loose contact method for catalytic soot oxidation experiments.

### 128 **3. Results and discussion**

129 The synthesized  $\text{BaRuO}_3$  has three crystallographic forms representative of the "hexagonal  
130 perovskite". These different forms depending of the pressure parameters, are known as the 9R, 4H  
131 and 6H layers. At ambient pressure,  $\text{BaRuO}_3$  has been found to adopt the 9-layers repeat sequence  
132 (chh) $_3$ . 9R- $\text{BaRuO}_3$  crystallizes in the Rhombohedral space group R-3m (unit cell  $a = 5.75 \text{ \AA}$  and  
133  $c=21.60 \text{ \AA}$ ). The structure consists of trimers of face sharing octahedra, which are joined via  
134 terminal corners to constitute a three-dimensional network [11]. The XRD analysis (Fig. 1)  
135 confirms the formation of single phase, crystalline  $\text{BaRuO}_3$  and infers that  $\text{BaRuO}_3$  can be easily  
136 synthesized by co-precipitation method with good purity and crystallinity. The BET-surface area

137 result of synthesized BaRuO<sub>3</sub> is observed to be 5 m<sup>2</sup>/g, which is in the expected range, considering  
138 the high synthesis temperature used, leading to sintering of material. The barium and ruthenium  
139 contents of the catalyst were determined using ICP-OES technique (Perkin–Elmer, Model Optima  
140 4100DV). Blank experiments were performed throughout the studies and majority of the  
141 experiments were repeated thrice and it was observed that the experimental error was within ±2%.  
142 The samples were dissolved in acid before the analysis. The BaRuO<sub>3</sub> sample was then studied for  
143 its thermal stability as RuO<sub>2</sub> suffers thermal loss due to the formation of volatile oxides. The post-  
144 heated material shows practically no change in the XRD pattern, thereby confirming the unchanged  
145 structure and crystallinity of the material, while practically no weight loss was observed during  
146 heating the materials on a TGA machine. It can therefore be inferred that Ru can be thermally  
147 stabilized as BaRuO<sub>3</sub> in perovskite structure, under the oxidative atmosphere.

### 148 **3.1. Catalytic activity**

149 Diesel particulate (soot) consists of carbon core associated with hydrocarbons including  
150 polyaromatic hydrocarbons (PAH) and nitro-PAH, sulfates, water, trace amounts of other metals  
151 [17]. The non-catalytic combustion temperature of soot generally exceeds 550 °C, however, this  
152 depends on various factors. Therefore, model soot/carbons are generally used for laboratory  
153 studies, which offer much better reproducibility than the natural soot. The model soot/carbons  
154 used in this study are activated carbon (for fixed bed evaluations) with following  
155 physicochemical properties: fraction of adsorbed hydrocarbons (5.2%), ash (<0.14%), C  
156 (94.2%), H (0.4%), N (0.3%), S (0.5%) and carbon black (Degussa S.A. Printex) for TGA based  
157 evaluations.

158 The carbon oxidation activity results for bare activated carbon using temperature  
159 programmed oxidation (TPO) are presented in **Fig. 2a**. These results suggest that the T<sub>i</sub>



160 (Temperature at which carbon oxidation initiated) of the non catalyzed oxidation of carbon starts  
161 above 400 °C and effective soot oxidation was observed only after 540°C with  $T_f$  (Temperature at  
162 which carbon oxidation completed) at 650 °C. TPO results for BaRuO<sub>3</sub> assisted activated carbon  
163 oxidation (Fig. 2b) suggest that the carbon oxidation with BaRuO<sub>3</sub> catalyst shows two peaks in  
164 the temperature range of 200–480 °C. This initial oxidation (first peak) can be attributed to the  
165 catalytic oxidation of soluble organic fraction (SOF) component, which is an exothermic  
166 reaction. The exothermic heat generated during oxidation of SOF fraction also leads to carbon  
167 oxidation, especially the carbon part in close contact with catalyst particles. Therefore, the first  
168 peak could be correlated to combined effect of SOF oxidation as well as carbon oxidation  
169 promoted by exothermic heat of SOF oxidation and that in closer contact with catalyst particles.  
170 The second peak appeared at 300 °C could be due to the release of CO<sub>2</sub> as a result of carbon  
171 oxidation without substantial SOF content and with relatively weaker contacts. The  $T_i$  and  $T_f$  of  
172 catalyst assisted soot oxidation were observed to be around 200 °C and 435 °C, respectively.  
173 These results show decrease in  $T_i$  value by about 200 °C and  $T_f$  by 215 °C with catalyst assisted  
174 carbon oxidation as compared to non-catalyzed activated carbon oxidation. Such results confirm  
175 high catalytic activity of BaRuO<sub>3</sub> in absence of NO<sub>x</sub>. Soot oxidation is usually facilitated by  
176 presence of NO<sub>2</sub> at low temperatures following the formation of NO oxidation to NO<sub>2</sub>. The  
177 observed lowering of carbon oxidation temperature in absence of NO<sub>2</sub> is therefore quite  
178 significant [18-23], and thus the present BaRuO<sub>3</sub> catalyst shows excellent catalytic activity  
179 considering it's very low surface area. This observation also support that the micro surface area  
180 is not very important in case of oxygen based soot/carbon oxidation considering the fact that  
181 both catalyst and a reactant are in solid state. There was practically no CO generation, which is  
182 sometimes present as a product of incomplete combustion. The XRD analysis of post-heated

183 sample at 900 °C does not show any change as compared to that of original material. This  
184 confirms the high thermal stability of BaRuO<sub>3</sub>, otherwise RuO<sub>2</sub> and Ru metal are well known to  
185 show thermal loss at such high temperatures in oxidative atmosphere. Such batch experiments  
186 using the air or simulated exhaust flow offer relatively more realistic conditions of catalyst use  
187 for DPF (Diesel particulate filter) regeneration as compared to thermo gravimetric analysis  
188 (TGA) based evaluations. The activation energy for catalyzed and non-catalyzed reactions was  
189 estimated by following the Ozawa method [15-16]. The activation energy values (Table 1) of  
190 catalyzed reactions under different conditions unambiguously substantiate the high catalytic  
191 activity of BaRuO<sub>3</sub> for carbon / soot oxidation using different feed gas mixtures.

192         A few mechanisms have been proposed for the catalytic soot/carbon oxidation using  
193 oxygen/air. Based on our previous extensive studies on soot oxidation reaction [20-23] as well as  
194 the kinetic analysis [24], we postulate that dissociative adsorption of oxygen on catalyst surface  
195 followed by its reaction with the solid soot/carbon at the soot-catalyst interface could be the  
196 possible mechanism for present perovskite composition. With this background, we have  
197 attempted the possibility of explaining high activity in relation to surface structure of this  
198 material as derived from crystallographic assumptions. Fig. 3 and Fig. 4 illustrate the possible  
199 rich oxygen–ruthenium surface chemistry. The ball model derived in the present study shows  
200 abundant population of Ru on –120 planes. We decided to study this plane with the hypothesis of  
201 needle particles (crystal growth along c axis), which is classically obtained for hexagonal  
202 stacking perovskite. Moreover, in case of BaRuO<sub>3</sub>, there is direct Ru-Ru interaction as compared  
203 to that of RuO<sub>2</sub>, which may favor dissociative adsorption of oxygen. However, another important  
204 factor for the relatively higher activity of BaRuO<sub>3</sub> may be the influence of adjacent Ba cation in  
205 perovskite structure. The basic character of Ba is expected to weaken the strength of Ru-O bond,

206 which facilitate the release of adsorbed oxygen. In this way, it is quite possible to explain the  
207 excellent catalytic activity of this material, while the material also shows a very important  
208 advantage of thermally stabilizing Ru in an oxide matrix.

#### 209 **4. Conclusions**

210 BaRuO<sub>3</sub> with perovskite structure can be easily synthesized using co-precipitation method.  
211 The catalytic material shows high catalytic activity for soot oxidation reaction as compared to most  
212 of the non-PGM (non-platinum group metals) based catalyst reported for direct soot oxidation,  
213 while it's activity is also comparable with PGM metal based catalysts. BaRuO<sub>3</sub> shows high soot  
214 oxidation activity under both flow type reactor conditions as well as TGA. 120 planes of BaRuO<sub>3</sub>  
215 are postulated to have abundant Ru atoms, which can facilitate the adsorptive dissociation of  
216 oxygen. This surface can also provide weak Ru-O interaction due to the presence of Ba, which may  
217 facilitate easy release of dissociated oxygen. It is also significant to achieve high thermal stability  
218 for ruthenium in an oxide matrix. The present catalytic studies of BaRuO<sub>3</sub> therefore suggest for the  
219 preparation of other similar metal ruthenates and study of their detailed catalytic and material  
220 properties. This metal ruthenate with perovskite structure shows potential for its applications in  
221 environmental catalysis. The high thermal stability of BaRuO<sub>3</sub> material is quite striking as this has  
222 been a major limitation with Ru based catalytic materials.

#### 223 **Acknowledgements**

224 This work was carried out under the DST-JSPS collaborative research project as well as  
225 under the research cooperation between CSIR-NEERI and University of Rennes, France. Thanks  
226 are also due to the Director NEERI for providing research facilities.

227

228

229 **References**

- 230 1. R. Prasad, B. Venkateswara Rao, A Review on Diesel Soot Emission, its Effect and  
231 Control, Bulletin of Chemical Reaction Engineering & Catalysis 5 (2010) 69 – 86
- 232 2. M. C. Somers, B.E. McCarry, F. Malek, J.S. Quinn, Reduction of Particulate Air  
233 Pollution Lowers the Risk of Heritable Mutations in Mice, Science 304 (2004)1008-1010
- 234 3. K. Yamazaki, T. Kayama, F. Dong, H. Shinjoh, A mechanistic study on soot oxidation over  
235 CeO<sub>2</sub>–Ag catalyst with ‘rice-ball’ morphology, J. Catal. 282 (2011) 289–298
- 236 4. S. Changsheng, P. J. McGinn, The effect of Ca<sup>2+</sup> and Al<sup>3+</sup> additions on the stability of  
237 potassium disilicate glass as a soot oxidation catalyst. Appl. Catal. B 138 (2013) 70– 78
- 238 5. A. Fihri, M. Bouhrara, U. Patil, D. Cha, Y. Saih, V. Polshettiwar, Fibrous Nano-Silica  
239 Supported Ruthenium (KCC-1/Ru): A Sustainable Catalyst for the Hydrogenolysis of  
240 Alkanes with Good Catalytic Activity and Life time, ACS Catal. 2 (2012) 1425–1431
- 241 6. A. Xiao, Z. Cai, T. Wang, Y. Kou, N. Yan, Aqueous-Phase Fischer–Tropsch Synthesis with  
242 a Ruthenium Nanocluster Catalyst, Angew. Chem. Int. Ed. 47 (2008) 746 –749.
- 243 7. J. Abmann, E. Loffler, A. Birkner, M. Muhler, Ruthenium as oxidation catalyst: bridging  
244 the pressure and material gaps between ideal and real systems in heterogeneous catalysis by  
245 applying DRIFT spectroscopy and the TAP reactor, Catal. Today 85 (2003) 235–249
- 246 8. M. Hasan, H.Park, J. Lee, H. Hwang. Improved thermal stability of ruthenium oxide metal  
247 gate electrode on hafnium oxide gate dielectric. Appl Phys Lett, 91(2007) 0335120-0335123
- 248 9. N.K. Labhsetwar, A. Watanabe, T. Mitsunashi, New improved syntheses of LaRuO<sub>3</sub>  
249 perovskites and their applications in environmental catalysis. Appl. Catal. B: Environ.  
250 40(2003) 21-30.

- 251 10. H. Over, M. Muhler, Catalytic CO oxidation over ruthenium—bridging the pressure gap,  
252 Prog. Surf. Sci 72 (2003) 3–17
- 253 11. D. Ming Han, X. Juan Liu, S. Hui Lv, H. Ping Li, J. Meng. Elastic properties of cubic  
254 perovskite BaRuO<sub>3</sub> from first-principles calculations. Physica B 405 (2010) 3117–3119
- 255 12. N.K. Labhsetwar, A. Watanabe, T. Mitsuhashi, US patent 0114752, 2002.
- 256 13. N.K. Labhsetwar, A. Watanabe, T. Mitsuhashi, Thermally stable ruthenium-based catalyst  
257 for methane combustion, J. Mol. Catal. 223 (2004) 217-223
- 258 14. N. Labhsetwar, P. Doggali, P. Chankapure ,D. Valechha, S. Lokhande, A. Watanabe, T.  
259 Mitsuhashi. La<sub>3.5</sub>Ru<sub>4.0</sub>O<sub>13</sub> Perovskite type Catalyst for Carbon Monoxide and  
260 Hydrocarbon Oxidation, Top.Catal.52(2009)1909-1914
- 261 15. T. Ozawa, Kinetic analysis of derivative curves in thermal analysis, J. Therm. Anal. 2  
262 (1970) 301-324
- 263 16. T. Ozawa, Estimation of activation energy by iso conversion methods. Thermochemica Acta  
264 203(1992)159-165
- 265 17. C. Lim, H. Einagab, Y. Sadaokac, Y. Teraoka, Preliminary study on catalytic combustion-  
266 type sensor for the detection of diesel particulate matter, Sensors and Actuat B- Chem, 160  
267 (2011) 463– 470
- 268 18. Q. Liang, X. Wu, D. Weng, H. Xu, Oxygen activation on Cu/Mn–Ce mixed oxides and the  
269 role in diesel soot oxidation, Catal. Today 139 (2008) 113-118.
- 270 19. X. Wu, F. Lin, D. Weng, J. Li, Simultaneous Removal of Soot and NO over Thermal  
271 Stable Cu–Ce–Al Mixed Oxides, Catal.comm. 9 (2008) 2428–2432.

- 272 20. M. Dhakad , S. Rayalu , P. Doggali , S. Bakardjiva , J. Subrt , D. Fino , H. Haneda , N.  
273 Labhsetwar,  $\text{Co}_3\text{O}_4\text{-CeO}_2$  mixed oxide-based catalytic materials for diesel soot oxidation,  
274 Catal. Today 132 (2008) 188–193
- 275 21. M. Dhakad, D. Fino, S. S. Rayalu, R. Kumar, A. Watanabe, H. Haneda, S. Devotta, T.  
276 Mitsuhashi, N. Labhsetwar, Zirconia supported Ru–Co bimetallic catalysts for diesel soot  
277 oxidation, Top. Catal 43(2007) 273-276
- 278 22. M. Dhakad, S.S. Rayalu, R. Kumar, P. Doggali, S. Bakardjiva, J. Subrt, T. Mitsuhashi, H.  
279 Haneda, N. Labhsetwar, Low Cost, Ceria Promoted Perovskite Type Catalysts for Diesel  
280 Soot Oxidation. Catal. Lett, 121(2008)137–143
- 281 23. P. Doggali, S.Kusaba, Y.Teraoka, P.Chankapure, S.Rayalu, N. Labhsetwar,  $\text{La}_{0.9}\text{Ba}_{0.1}\text{CoO}_3$   
282 Perovskite type Catalysts for the Control of CO and PM Emissions, Cata. Comm.11 (2010)  
283 665–669.
- 284 24. W. F Shangguan, Y.Teraoka, S. Kagawa, Kinetics of soot— $\text{O}_2$ , soot—NO and soot— $\text{O}_2$ —  
285 NO reactions over spinel-type  $\text{CuFe}_2\text{O}_4$  catalyst, Appl. Catal. B, 12(1997) 237-247.  
286  
287  
288  
289  
290  
291  
292  
293  
294  
295

296 **Figures:**

297 Fig. 1: XRD Pattern for BaRuO<sub>3</sub>

298 Fig. 2a: Temperature Programmed Oxidation results for carbon oxidation: bare activated carbon

299 Fig. 2b: Temperature Programmed Oxidation Results for carbon oxidation: activated carbon  
300 with BaRuO<sub>3</sub> catalyst.

301 Fig. 3: Ball model of the BaRuO<sub>3</sub> (-120) surface

302 Fig. 4: Projection along [010] of the (-120) surface

303

304

305

306

307

308

309

310

311

312

313

314

315

316

317

318

319

320

321

322

323

324

325

326

327

328

329

330

331

332

333

334

335

336

337

338

339

340

341

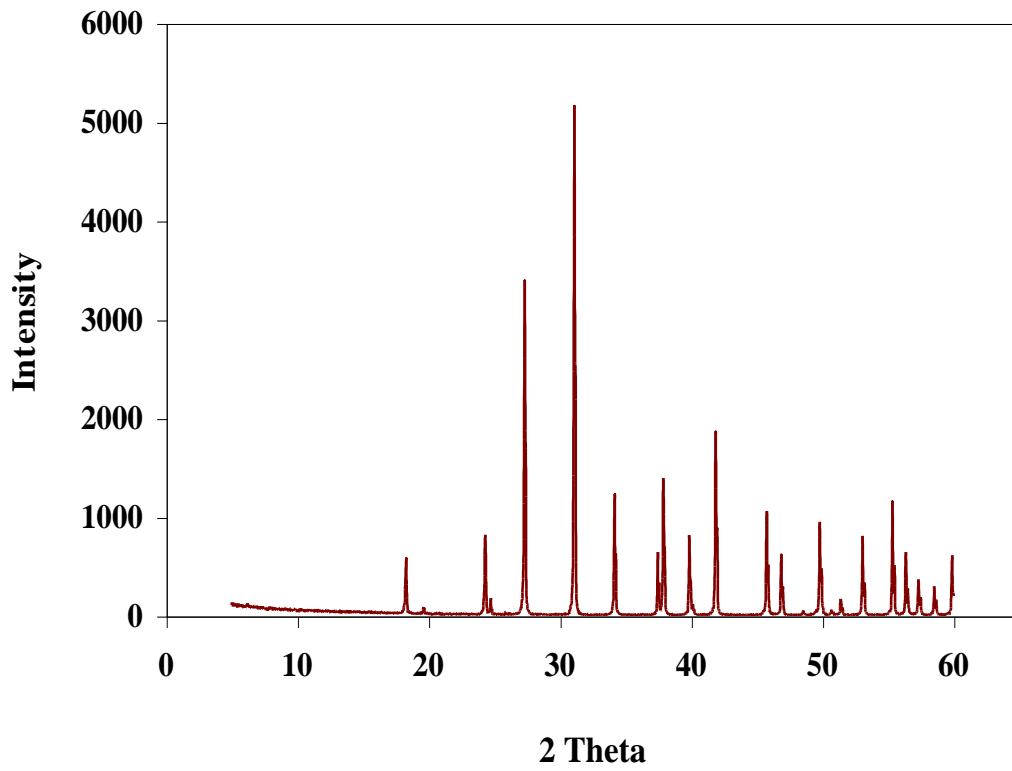


Fig.1



342

343

344

345

346

347

348

349

350

351

352

353

354

355

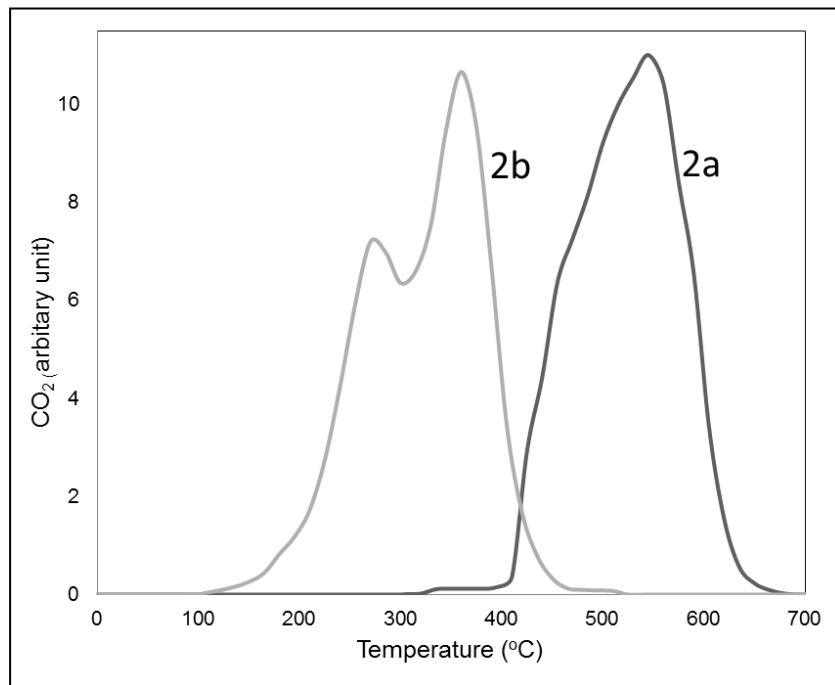
356

357

358

359

360



361 **Fig. 2a & Fig. 2b**

362

363

364

365

366

367

368

369

370

371

372

373

374

375

376

377

378 **Fig. 3**

379

380

381

382

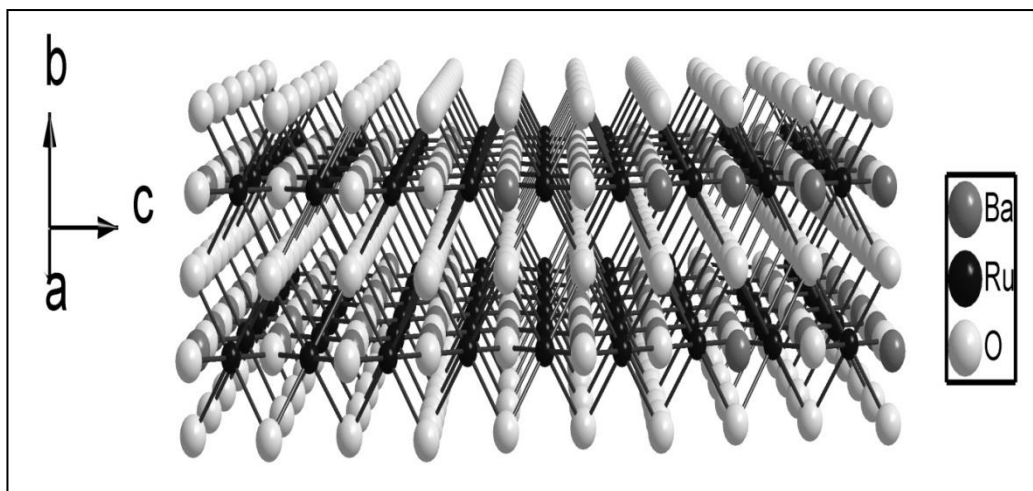
383

384

385

386

387



388

389

390

391

392

393

394

395

396

397

398

399

400

401

402

403

404

405

406 **Fig. 4**

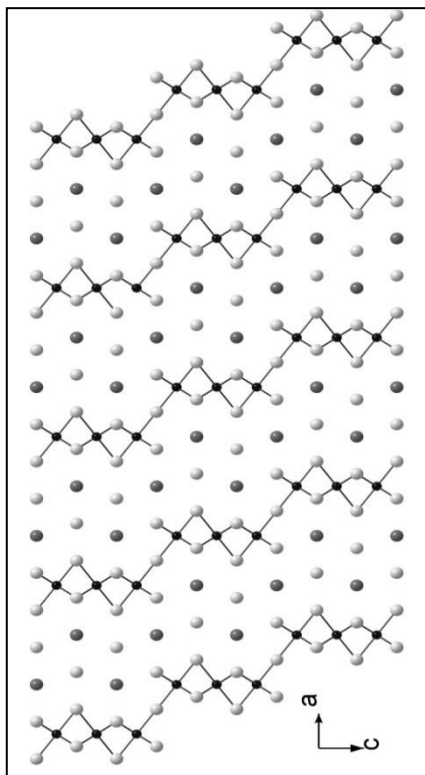
407

408

409

410

411



412

<b>Sample</b>	<b>Activation Energy kJ/mol</b>		
<b>Bare carbon black</b>	150 (Air flow)	165 (12% O <sub>2</sub> )	160 (12% O <sub>2</sub> +10% CO <sub>2</sub> )
<b>Carbon black +BaRuO<sub>3</sub></b>	120 (Air flow)	135(12% O <sub>2</sub> )	130(12% O <sub>2</sub> +10% CO <sub>2</sub> )

413

414 **Table 1: Activation energy values (Ozawa Plot), kJ/mol**